TOWARDS AN OBJECT-BASED DETECTION OF EARTHQUAKE DAMAGED BUILDINGS

T. T. Vu [a,1], M. Matsuoka [a], F. Yamazaki [b]

[a] Earthquake Disaster Mitigation Research Center (EDM), National Res. Inst. for Earth Science and Disaster Prevention, 1-5-2 Kaigandori, Wakinohama, Chuo-ku, Kobe 651-0073, Japan - (thuyvu, matsuoka)@edm.bosai.go.jp
[b] Department of Urban Environment Systems, Faculty of Engineering, Chiba University, 1-33 Yayoi-cho, Inage-ku, Chiba 263-8522, Japan - yamazaki@tu.chiba-u.ac.jp

Commission VII, WG VII/5

KEY WORDS: Earthquakes, Urban area, Damage detection, Object-based extraction, Very high resolution satellite image.

ABSTRACT:

As the spatial resolution of satellite images has been constantly improved, it is possible to quickly capture a detailed damage map after a catastrophe using remote sensing techniques. The commercialisation of very high spatial resolution (VHR) satellite images such as IKONOS and QuickBird especially allows the detection of individual buildings or a block of buildings. However, a better spatial resolution image requires a more complicated processing. A VHR image possesses much more information than a coarser one. Pixel-based and texture-based methods, which are successfully used for coarse spatial resolution images, show certain limitation in processing VHR satellite images. Currently, visual interpretation of VHR images for building damage detection is the most reliable method. This manner is obviously time-consuming and requires experienced interpreters.

To ease the task, this study tries to develop a more automated interpretation method. Scale-space is generated based on the theory of area morphology to analyse the spectral information in a morphological framework. Across the scale-space, the processing mimics the human perception by moving upwards from a coarse scale to finer ones and comparing between the pre-event and post-event images. Non-damaged buildings are extracted firstly and the results infer the damage ones. A pair of QuickBird scenes acquired over the city of Boumerdes, which was one of the most heavily-damaged areas due to the Algeria earthquake on May 21, 2003, and a pair of QuickBird scenes acquired over the city of Bam, Iran, which was damaged due to the Iran earthquake on December 26, 2003, are used for demonstration of the method. Both cases, i.e. dense distribution of buildings in Bam city and sparse distribution of buildings in Boumerdes show the successful extraction of damaged buildings. It proves that the proposed method is very promising to be widely employed. More analyses to categorise the damaged buildings to a suitable damage scale and implementation of the method will be conducted in a future study.

1. INTRODUCTION

For decades, remote sensing techniques have played an important role in disaster damage assessment. Providing the geo-spatial data over a large area, they are the most capable technique used in post-disaster response, especially for the hard-hit and difficult-to-access areas. Recent catastrophes have been observed and captured by various remote sensors on different space-borne or airborne platforms. It triggers a great employment of remote sensing techniques in post-disaster response. Focusing on the employment of remote sensing in earthquake damage detection, many researches and implementations have been carried out after several recent big earthquakes such as the 1995 Kobe, Japan earthquake (Matsuoka and Yamazaki, 1999), the 1999 Kocaeli, Turkey earthquake (Eguchi et al. 2000; Estrada et al. 2000), the 2001 Gujarat, India earthquake (Mitomi et al. 2001; Saito et al. 2004), the 2003 Bam, Iran earthquake (Vu et al. 2005; Yamazaki et al. 2005). Either optical or radar, images at different resolutions have been used. The availability of higher resolution images these days allows the interpretation of damage scale of each building block or even each individual building rather than overall damage distribution and damage extent. Both visual and automated interpretations are used to derive the damage information from remotely sensed images.

At the lowest level of processing, image processing deals with pixels. Each pixel possesses the grey value which represents the spectral reflectance at its location. Based on that, a vast amount of "pixel-based" algorithms were developed. "Texture-based" algorithms are higher level of processing, which analyse different kinds of relationship among the neighbours of each pixel. These two types of processing have been successfully used for coarse resolution images like Landsat and ERS (Matsuoka and Yamazaki, 1999; Eguchi et al., 2000; Estrada et al., 2000). The reason is that coarse images do not provide detailed information. A pixel itself might be a mixture of different objects. Therefore, pixel or texture information is the reasonable cue for the detection and extraction of damage extent and distribution. Airborne-based images and very high resolution (VHR) satellite images such as QuickBird and IKONOS, which provide highly detailed information, require much more complicated processing. Those pixel-based and texture-based methods developed could be used with airborne-based images (Mitomi et al. 2001) and VHR satellite images (Vu et al. 2005). However, it was unable to exploit all

[1] Corresponding author

possessed information in a high resolution image. The visual interpretation, which obviously is time-consuming and requires experienced interpreters, has been a more reliable method (Yamazaki et al. 2005). To automate the interpretation, "object-based" image processing should be developed.

Objects presented on an image possess the scale property. Exploitation of scale in image processing, in fact, mimics the human perception. Human perception ignores the details and groups the pixels into an object at a specific scale of observation. Linear scale-space has been well-developed in feature extraction and visualisation (Lindeberg, 1993). To overcome the distortion problem at a coarser scale by the linear scale-space, which generates difficulty in linking across the scale-space, non-linear scale space is proposed. Non-linear scale space keeps the main properties of a scale-space like luminance conservation, geometry, or morphology (Petrovic et al. 2004). Generally, it performs a partition of an image into isolevel sets at each scale and links them with the closest one in the next scale. The proposed method presented in this paper employs area morphology (Vincent, 1992) to construct the nonlinear scale-space. Its theory is presented in Section 2. A newly proposed damage detection method is introduced in Section 3. It is followed by two tests with QuickBird images (Section 4) and conclusion, discussion of further developments (Section 5).

2. AREA MORPHOLOGICAL FILTERING

As introduced by Vincent (1992), area opening filtering removes the components with area smaller than a parameter *s* from a binary image. Similarly, area closing filtering fills the holes with area smaller than a parameter *s*. The binary area opening is defined as follows; Let set X is a subset of set $M \subseteq R^2$ and $\{X_i\}$ is all the connected components of X. The area opening of parameter s ($s \geq 0$) of X is the union of the connected components of X with an area greater than s:

$$\gamma_s^a(X) = \bigcup\{X_i \mid i \in I, Area(X_i) \geq s\} \quad (1)$$

The area closing of parameter s ($s \geq 0$) of X is then defined as:

$$\phi_s^a(X) = \left[\gamma_s^a(X^C)\right]^C \quad (2)$$

where X^C denotes the complement of X in M.

Vincent (1992) then extended the definition of binary area opening or closing to greyscale area opening or closing. A greyscale image can be defined as a mapping $f : M \to R$.

The greyscale opening of f is given by:

$$(\gamma_s^a(f))(x) = \vee\{h \leq f(x) \mid x \in \gamma_s^a(T_h(f))\} \quad (3)$$

where $\vee$ stands for supermum, i.e. a lowest upper bound, and T_h is the threshold of f at value h.

$$T_h(f) = \{x \in M \mid f(x) \geq h\} \quad (4)$$

In other words, the image M is firstly threshold with all the possible h and the binary opening $\gamma_s^a(T_h(f))$ is found. Subsequently, $\vee$ is applied to all the recently found $\gamma_s^a(T_h(f))$. It is similarly extended to greyscale closing by duality. Area morphological filtering does not depend on the shape of structural elements as the conventional ones. Therefore, it can effectively remove noise and simultaneously retain thin or elongated objects.

3. DAMAGE DETECTION METHOD

There are currently two damaged building detection approaches: solely use the post-event image or detect the changes between the pre-event and post-event images. The former like Mitomi et al. (2001) detects building damage through the distribution of edges of buildings and/or debris. Such methods can detect only the location of the damage. Till now, there is no detailed report on the relationship between the detected indexes and the damage levels. The latter like Estrada et al. (2000) follows the scheme of change detection. More information about the damage can be expected. However, the seasonal or man-made changes must be excluded afterwards. To detect more detailed damage information, our proposed method follows the second approach. Damage detection is interpreted through the changes of building objects. The building objects are firstly extracted from both the pre-event and post-event images across the scale-space prior to the comparison. The scale-space is generated based on area morphology (Section 2) as described in the following sub-section.

3.1 Scale space

Applying area opening followed by area closing with a parameter *s*, named *AOC* operator, on an image is hence, like flattening this image by parameter *s*. This performance segments an image into the flat zones of similar intensity or isolevel sets, in other words. Therefore, a scale-space can be generated by iteratively applying *AOC* with increasing *s*. The desirable properties of a scale space like fidelity, causality, Euclidean invariance, are hold by *AOC* scale-space (Acton and Mukherjee, 2000). Theoretically, the scale-space is generated by an infinite number of scales. For the discrete dimension of an image, the number of scales increases one each as a window (area) size increases from one pixel to an image size. However, it is time-consuming to concern all the area values. Practically, a scene contains a limited number of sizes. Horizontal and vertical granulometry analyses (Vincent, 1994) are carried out to find the potential patterns contained in an image. The local maximum found in horizontal and vertical dimensions can be used to compute the possible areas of objects in the image.

Across the scale space from a coarse scale to finer ones, an object is created and split. To extract the objects from the scale-space of a greyscale image, the linking trees of objects must be formed across the scale-space. On each scale, an object might have its parent on previous coarser scale and its children on next finer scale. The similarity of object's intensity is the criterion to determine the hierarchical relationship. If an object's intensity is much different from that of the big object which it falls into, the scale on which it is created is the root of the linking tree. Subsequently, an object can be extracted on its root scale along with its associated linking tree.

Figure 1 demonstrates the idea of linking object across the scale-space. Let assume that we are considering three-level scale-space with *S1* the coarsest and *S3* is the finest. On the current scale *S2*, there are two newly created objects named *A* and *B*. While *A* has similar intensity to the bigger one at scale *S1*, *B* has different intensity. As a result, *B* can be extracted on this scale *S2* with its two-level tree and *A* is associated with its father on *S1* and two children on *S3* to form a three-level tree.

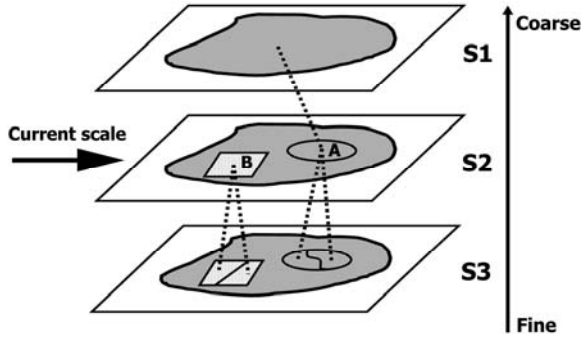

Figure 1. Objects linking across the scale space.

3.2 Damage detection

Practically, multi-spectral images are used rather than greyscale ones. The scale-space scheme presented above for greyscale images is applied to each band. The area parameters can be derived by granulometry analysing the first component of Principle Component Analysis (PCA). Subsequently, the spectral signatures are grouped and assigned the class indexes by K-mean clustering (Tou and Gonzalez, 1974). Figure 2 illustrates the results of clustering on 3 scales, s = 50, 200 and 1000 associated with the original true colour composite (TCC) image (Figure 2a) for reference. A relational database is generated to link the class indexes across the scale-space to linguistic variables which represent the land-cover types such as water body, vegetation, shadow, building roof, etc. This database will be used in the process of linking and segmentation of the objects across the scale-space.

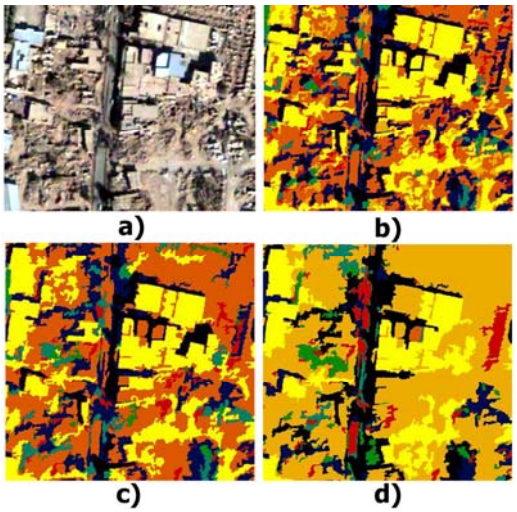

Figure 2. a) Original TCC image and the results of K-mean clustering on scales b) s = 50, c) s = 200 and d) s = 1000.

All objects are linked and the relationships are stored in a new database. However, focusing on building features, other classes can be ignored in the extraction. The linking is started at the finest scale. The attributes of each object are

- SCALE: the current scale in which it exists,
- ID: the identified number on the current scale,
- AREA: object's area,
- X0, Y0: image coordinates of the starting point of an object,
- X, Y: image coordinates of the centroid; this point will be shifted to an arbitrary location inside the object if it is concave,
- SHAPE: to indicate the object is convex or concave,
- SPECTRAL: spectral class,
- SUPERID: the identified number of the object's father on the next coarser scale, this number equals 0 if the scale is the root of this object.

The criterion to determine the relationship between an object and its potential father is the spectral class. Subsequently, a building can be extracted on its root scale. Figure 3 shows the extracted buildings from a portion of the post-event image acquired over Bam city, Iran. Three coarsest scales are used for demonstration. Three scales s = 200, 500 and 2000 are combined in Red, Green and Blue channels, respectively. Obviously, it shows the retained buildings after the earthquake.

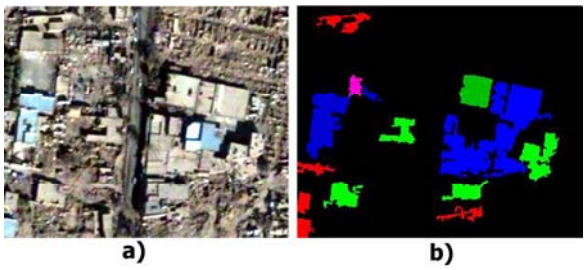

Figure 3. a) Original TCC image and b) extracted results on scales s = 200 (Red), s = 500 (Green) and s = 1000 (Blue).

Building objects extracted from the pre-event and post-event images are compared to find out damage. Currently, the development of the method has been reached the step of finding the exact location of the collapsed buildings. It is inferred by logical comparison on the existence of building objects before and after a catastrophe. It should be noted that the extraction of a building object is actually the extraction of its roof. The looking angles of the sensors when capturing the pre-event and post-event images might be different. As a result, the buildings lean to different directions in comparison between the pre-event and post-event images. To compare the existence of building objects, a systematic shifting the building roof's polygon is required and more complicated comparison must be developed. Further classification of the damage level by object comparison will be a next development. An additional step to exclude other changes not due to the catastrophe will also be included.

4. TESTING RESULS

Two tests were carried out for Boumerdes city, Algeria and Bam city, Iran. The former is a typical city with sparsely distributed buildings and the latter is a very dense city, on the contrary. Boumerdes was one of the most heavily-damaged areas due to the earthquake on May 21, 2003. Its pre-event QuickBird scene was about one year before the event (April 22, 2002) and its post-event one was two days after the event (May 23, 2003). In the same year, another strong earthquake occurred beneath the city of Bam, Iran, on December 26. The test used QuickBird scenes observed the city on September 30, 2003 and January 3, 2004, respectively. Figure 4 shows the extracted portions of those images for testing. They are typical representatives of building alignments in these cities.

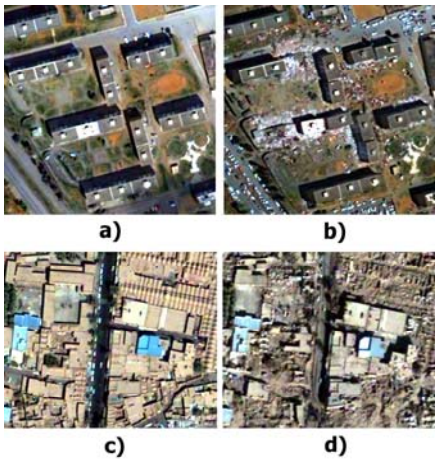

Figure 4. Extracted portions for testing of Bourmedes a) pre-event, b) post-event images and Bam c) pre-event and b) post-event images.

Since the distributions of buildings in two areas are very different, the images of two areas present very different situations. Few building shadow can be observed in the pre-event image of Bam. However, the very good point of Bam images is a quite clear difference of building's spectral signatures in comparison with others. The building objects were successfully extracted from the Bam images as shown in Figures 5a and 5b. Colour code is given according the ID and SCALE of each extracted building. The locations of damaged buildings were also detected as bright areas in Figure 5c. There were several commission errors caused by small objects like cars and the small difference of sensor looking angles. Those errors can be removed by opening morphological filtering as shown in Red in Figure 5d.

As building features in images of Boumerdes possess very similar spectral signatures as other objects like streets, they could not be extracted by using solely spectral information. The size property, which was presented through the scale space, was also not enough because many other objects had the same size. Fortunately, the shadows of building features were presented very clearly. This property should be included as an attribute of the building objects in the case when this kind of object can be successfully extracted. For the case of Boumerdes images, extraction of shadow objects for damage detection might be more effective than extraction of building objects. The extracted results are shown in Figure 6. They are well separated because of the sparse distribution of the buildings.

Following our previous study (Vu et al. 2004), damage can be indirectly detected through the comparison of shadow's lengths in the longitudinal and transverse directions of the buildings between the pre-event and post-event images. Four damage building blocks were detected and named A, B, C and D. While A is a commission error due to the shadow of cloud, other three blocks were correctly detected as they were heavily damaged. There is also an omission error, which was the slightly damaged building block locating at the top-right of the image. Through these two tests, it is recommended to include the shadow of buildings, the lengths in the longitude and transverse directions as the attributes of building objects. The indirect detection of shadow behaviour is a good solution as the spectral signatures of building objects show less discrimination in comparison with others.

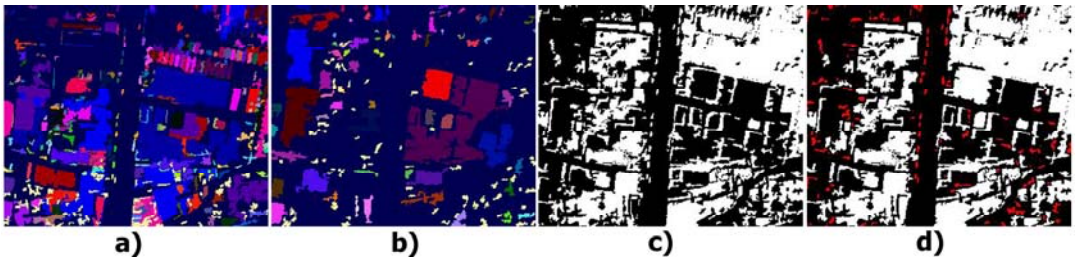

Figure 5. Extracted buildings from Bam images: a) pre-event, b) post-event with dark blue for background and location of damaged buildings: c) before filtered, d) after filtered.

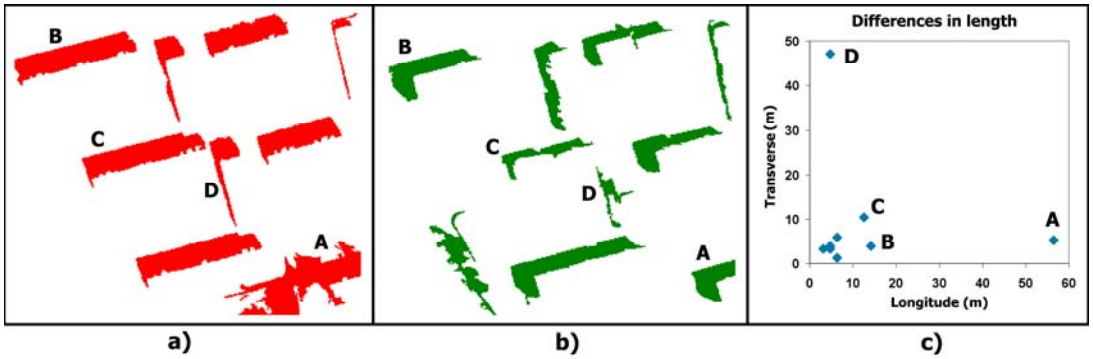

Figure 6. Extracted shadows from Boumerdes images: a) pre-event, b) post-event and c) comparison of shadow lengths

5. CONCLUSIONS

An object-based detection method of damaged buildings was proposed. Its implementation has been accomplished and several tests have been carried out for verification of the algorithms. This method was built on the theory of area morphology to extract building objects. Subsequently, several extracted properties like spectral, size, hierarchical relationship, etc. were used comparing the existences of a building before and after a catastrophe. As the spectral signature is a main factor, if these of the building objects show very similar to others, the shadow of buildings can be used as an indirect damage detection method. Testing results showed good agreement with the results by visual interpretation**.** More complicated comparison of building objects will be concerned in further development for classification of damage levels and removal of other changes not due to the concerned disaster. In order to do that, more context information should be included such as building orientation, classification of structure types, using building objects, their shadow objects and perhaps, additional sources.

REFERENCES

Acton, S. T., and Mukherjee, D. P., 2000. Scale space classification using area morphology. *IEEE Transactions on Image Processing*, 9 (4), pp. 623-635.

Eguchi, R.T., Huyck, C.K., Houshmand, B., Mansouri, B., Shinozuka, M., Yamazaki, F. and Matusoka, M., 2000. The Marmara Earthquake: A View from space: The Marmara, Turkey Earthquake of August 17, 1999: Reconnaissance Report. Technical Report MCEER-00-0001: pp. 151-169.

Estrada, M., Yamazaki, F., and Matsuoka, M., 2000. Use of Landsat Images for the Identification of Damage due to the 1999 Kocaeli, Turkey Earthquake. In: *Proceeding of 21st Asian Conference on Remote Sensing*, November 2001, Singapore, pp. 1185-1190.

Lindeberg, T., 1993. Discrete Derivative Approximations with Scale-Space Properties: A Basis for Low-Level Feature Extraction. *Journal of Mathematical Imaging and Vision*, 3 (4), pp. 349-376.

Matsuoka, M. and Yamazaki, F., 1999. Characteristics of Satellite Images of Damaged Areas due to the 1995 Kobe Earthquake. In: *Proceedings of Second Conference on the Applications of Remote Sensing and GIS for Disaster Management*, The George Washington University, CD-ROM, 1999.

Mitomi, H., Saita, J., Matsuoka, M. and Yamazaki, F., 2001. Automated Damage Detection of Buildings from Aerial Television Images of the 2001 Gujarat, India Earthquake. In *Proceedings of the IEEE 2001 International Geoscience and Remote Sensing Symposium*, IEEE, CD-ROM, 3p.

Petrovic, A., Divorra Escoda, O., and Vandergheynst, P., 2004. Multiresolution segmentation of natural images: From linear to non-linear scale-space representations. *IEEE Transactions on Image Processing*, 13 (8), pp. 1104-1114.

Saito, K., Spence, R.J.S., Going, C., and Markus, M., 2004. Using high-resolution satellite images for post-earthquake building damage assessment: a study following the 26 January 2001 Gujarat Earthquake. *Earthquake Spectra*, 20 (1), pp. 145–169.

Tou, J.T. and Gonzalez, R.C., 1974. *Pattern Recognition Principles*, Reading, Massachusetts: Addison-Wesley Publishing Company.

Vincent, L., 1992. Morphological Area Opening and Closings for Greyscale Images. In: *Proceeding NATO Shape in Picture workshop*, Driebergen, The Netherlands, Springer-Verlag, pp. 197-208.

Vincent, L., 1994. Fast Grayscale Granulometry Algorithms. In *Proceeding EURASIP Workshop ISMM'94, Mathematical Morphology and its Applications to Image Processing*, Fontainebleau, France, pp. 265-272.

Vu, T.T., Matsuoka, M., and Yamazaki, F., 2004. Shadow Analysis in Assisting Damage Detection due to Earthquakes from QuickBird Imagery. *International Archives of Photogrammetry and Remote Sensing*, Vol. XXX IV, Part B7, Istanbul, Turkey, pp. 607- 610.

Vu, T.T., Matsuoka, M., and Yamazaki, F., 2005. Detection and Animation of Damage in Bam City Using Very High-resolution Satellite Data, *Earthquake Spectra*, Special Issue, 2003 Bam, Iran, Earthquake Reconnaissance report, EERI (in press).

Yamazaki, F., Yano, Y., and Matsuoka, M., 2005. Visual Damage Interpretation of Buildings in Bam City Using QuickBird Images, *Earthquake Spectra*, Special Issue, 2003 Bam, Iran, Earthquake Reconnaissance report, EERI (in press).

ACKNOWLEDGEMENTS

The Quickbird images used in this study are owned by Digital Globe, Inc. They are licensed and provided by Earthquake Engineering Research Institute (EERI), Oakland, California, USA.